ized state by the alternating field technique. Figure 5(D) shows such an occurrence. Moreover, the film can be carried through a step-by-step magnetization reversal if the coercing field is controlled with extreme care, and the change of the magnetization pattern proceeds in a fashion unlike any that we have seen reported. This film, evaporated under the same field conditions as the thicker specimens, retains the same longitudinal anisotropy. However, in the reversal process, a small island of altered magnetization edged by jagged "grassy" walls first appears across the center area. With increasing longitudinal field the irregular walls move along the field direction toward the two edges of the film. Figure 8 depicts four steps in this type of reversal. The poorer quality of the photographs results from the fact that this film is semitransparent and reflections from the unmetalized surface of the glass substrate are appreciable. There is also some evidence to suggest that the dark and lighter regions in these pictures may represent something other than strictly antiparallel directions of magnetization, but only photographs taken under controlled photometric conditions and analyzed by quantitative photometric methods can accurately decide this point. The observations further showed that this type of magnetization reversal also occurs in the 1500 A specimen but not in any of the thicker ones, and thus may well be a characteristic associated with small thickness.

It should be mentioned that the 10 000 A and 20 000 A films failed to show a domain structure. It is possible that these two specimens exceed in thickness Kittel's critical value for this alloy, provided that there exists a preferred direction of magnetization normal to the film surface induced by stress or other causes. On the other hand, investigation of evaporated films thinner than 500 A becomes increasingly difficult by the reflection method. Observation of very thin specimens by transmission appears promising, and we are at present undertaking a study of the practicability of such a technique.

PHYSICAL REVIEW VOLUME 104, NUMBER 3 NOVEMBER 1, 1956

# Lattice-Scattering Mobility of Holes in Germanium

H. EHRENREICH, *General Electric Research Laboratory, Schenectady, New York*

AND

A. W. OVERHAUSER, *Department of Physics, Cornell University, Ithaca, New York*

(Received April 23, 1956)

The lattice-scattering mobility of holes in germanium is calculated by using the transition probabilities for scattering by acoustical and optical phonons derived in an earlier paper, in which both the rigid- and deformable-ion models were used to determine the interaction between holes and the lattice. Coupled Boltzmann equations are considered, describing the distribution of carriers under the influence of an electric and phonon field in the two valence bands of germanium, degenerate at $k=0$. The results involve two previously described constants $C_1$ and $C_4$ which are treated as arbitrary parameters. Results are presented for several sets of these parameters and also for values of the temperature $\Theta=300°K$ and $500°K$ which might correspond to the fundamental optical frequency of the germanium lattice. The curves, $\log\mu$ *vs* $\log T$, closely resemble straight lines over the lattice-scattering range. It is possible to find values of $C_1$ and $C_4$ for both rigid- and deformable-ion models which agree well with the observed mobility if $\Theta=300°K$ but not if $\Theta=500°K$. The question as to whether these values of $C_1$ and $C_4$ are correct is not considered in this paper.

## 1. INTRODUCTION

THE transition probabilities for scattering of holes by acoustical and optical phonons in the two germanium valence bands degenerate at $\mathbf{k}=0$ have been calculated in an earlier paper.[1] In this treatment, the electron-phonon interaction Hamiltonian was seen to be separable into two parts: the first arises from the vibrations of the unit cell as a whole, and the second from the relative motion of the two atoms in the unit cell of the germanium lattice. The matrix elements for scattering were expressible in terms of two constants, $C_1$ and $C_4$, associated, respectively, with the two parts of the interaction Hamiltonian. The terms in $C_1$ describe the interaction of holes with acoustical vibrations; the terms in $C_4$ describe the interaction with optical and acoustical vibrations. The wave functions used to calculate the matrix elements were determined from the $\mathbf{k}\cdot\mathbf{p}$ and spin-orbit perturbations, the valence bands near $\mathbf{k}=0$ being described by spherical surfaces of constant energy and a parabolic relationship between energy and wave number, $E_s=(\hbar^2/2m_s)k^2$, where $m_s$ is the cyclotron resonance effective mass corresponding to one of the two degenerate bands.

For the terms in $C_1$ the scattering was treated using both deformable and rigid-ion models. The transition probabilities were seen to have a pronounced angular

[1] H. Ehrenreich and A. W. Overhauser, Phys. Rev. **104**, 331 (1956); hereafter referred to as I.

distribution for the scattering processes caused by absorption and emission of longitudinal and transverse phonons. These angular distributions are quite different for the two models. For the deformable-ion model, the heavy holes are scattered predominantly in the forward direction and the light holes in the backward direction, whereas the opposite is true for the rigid-ion model. In the former case, the scattering resulting from transverse and longitudinal modes is about equally important, in the latter case scattering by transverse modes is less important. The angular distribution associated with the terms in $C_4$ is simpler: the scattering is symmetric about the angle 90°. This simplicity results from the fact that an initial state along a [100] direction was assumed in calculating the matrix elements, an approximation that could be circumvented in treating the terms in $C_1$ by choosing the atomic cells spherical. This approximation could not be used in calculating the remaining terms since the constant $C_4$ vanishes in this approximation. The interference between the acoustical terms in $C_1$ and $C_4$ was not considered.

In the present paper, the preceding results will be used to calculate the mobility for a temperature range extending roughly between 100°K and 300°K where lattice scattering is the predominant scattering mechansim. Section 2 will be concerned with the transport calculations necessary to obtain the mobility. The results will be analyzed and discussed in Sec. 3.

## 2. TRANSPORT CALCULATIONS

The central problem of this section is the calculation of the current density,

$$j=-(e/4\pi^3)\sum_s \int \mathbf{v}_s f_s(\mathbf{k}_s) d^3k_s, \tag{1}$$

arising from carriers in both bands $s=1,2$ under the influence of the electric field $\mathcal{E}$ and the various kinds of phonon scattering considered in the earlier paper. The carriers have a velocity

$$\mathbf{v}_s=(\mathrm{grad}_k E_s)/\hbar. \tag{2}$$

Their distribution in $k$ space is described by the function $f_s(k_s)$, which is obtained as a solution of the Boltzmann equation. From Eq. (1) the mobility can be computed by use of the relationship

$$\mu=j/ne\mathcal{E}, \tag{3}$$

where $n$ is the density of current carriers.

Since in the present problem we are concerned with two interacting bands, we shall have to treat two coupled Boltzmann equations. Each equation states that the total rate of change with respect to time of the distribution function describing that band, due to the applied electric field and phonon scattering for all modes and polarizations, is zero.

Let $(\partial f_s/\partial t)_{\nu,r}{}^P \equiv (\dot{f}_s)_{\nu,r}{}^P$ be the rate of change of the distribution of electrons in band $s$ due to holes in this band, having wave number $k_s$, being scattered into some state $k_r'$ in band $r$, and in addition that due to electrons in band $r$, being scattered into the state $k_s$ by a process of type $\nu$ involving phonons having polarization $P$, as defined by Eq. (4.34) of I. In addition, define $(\dot{f}_s)_F$ as the rate of change of the distribution of holes in band $s$ produced by the applied field $\mathcal{E}$. Then the Boltzmann equation for band $s$ can be written in the form

$$(f_s)_F+\sum_{\nu=1}^{3}\sum_P\sum_{r=1}^{2}(f_s)_{\nu,r}{}^P=0. \quad (s=1,2). \tag{4}$$

We postulate a solution of the form

$$f_s(k_r)=f^0(E_r)+[df^0(E_r)/dE_r]a_s(E_r)\cos\theta_r, \tag{5}$$

which will be shown to satisfy Eq. (4) for the scattering terms considered here. In Eq. (5), $f^0$ is the equilibrium distribution describing the carriers when no external field is applied, and $\theta_r$ is the angle between the direction of $k_r$ and the field. The equilibrium distribution is the same in both bands. The current carriers obey Boltzmann statistics so that

$$f^0(E)=be^{-E/KT}, \tag{6}$$

where

$$b=4\hbar^3 n_s(\pi/2m_sKT)^{\frac{3}{2}} \quad (s=1,2). \tag{7}$$

Here $n_s$ is the density of carriers in band $s$. Since $b$ in Eq. (6) must be the same for both bands, it follows that $n_1/m_1{}^{\frac{3}{2}}=n_2/m_2{}^{\frac{3}{2}}$. With this relationship and Eq. (4.20), we can express $b$ in terms of $n=n_1+n_2$ and $\alpha=m_2/m_1$ as follows:

$$b=4\hbar^3 n(\pi/2m_1KT)^{\frac{3}{2}}/(1+\alpha^{\frac{3}{2}}). \tag{8}$$

We suppose that the electric field is applied along the $z$ direction. Substitution of the group velocity (2) and Eq. (5) into (1) yields

$$j=[2^{\frac{3}{2}}ne/3\pi^{\frac{1}{2}}m_1{}^{\frac{3}{2}}(KT)^{5/2}(1+\alpha^{\frac{3}{2}})]\times\sum_s m_s\int_0^\infty Ee^{-E/KT}a_s(E)dE. \tag{9}$$

The main part of the calculation will consist of determining the coefficients $a_s(E)$ from Eqs. (4). If there were but one band, $a_s(E)$ would be proportional to the relaxation time $\tau$ as can be shown by a comparison of (5) with the solution of the Boltzmann equation in the relaxation time approximation, which gives

$$\tau(E)=(m_1/2E)^{\frac{1}{2}}a_1(E)/e\mathcal{E}. \tag{10}$$

We shall now turn to the problem of evaluating the $(\dot{f}_s)_{\nu,r}{}^P$. For this purpose, we use the polar coordinate system of Fig. 1, and the relationship

$$\cos\theta_r=\cos\theta_s\cos\beta-\sin\theta_s\sin\beta\cos\phi. \tag{11}$$

In terms of this coordinate system, the density of final states in a small region about $k_r'$ is given by

$$\rho_r dE=(V/8\pi^3)d^3k_r'=-(Vm_rk_r'/8\pi^3\hbar^2)dx\,d\phi\,dE, \tag{12}$$

where we have written $x=\cos\beta$. An approximate mathematical statement of the definition for $(f_s)_{\nu,r}{}^P$ is obtained with the aid of the transition probabilities defined by Eq. (4.34) of I:

$$(f_s)_{\nu,r}{}^P=(2\pi/\hbar)(Vm_rk_r'/8\pi^3\hbar^2)\int_0^{2\pi}d\phi\int_{-1}^{+1}dx$$
$$\times\{f_r(k_r')[\mathcal{W}_\nu{}^P(s,n+1;r,n)+\mathcal{W}_\nu{}^P(s,n-1;r,n)]$$
$$-f_s(k_s)[\mathcal{W}_\nu{}^P(r,n+1;s,n)+\mathcal{W}_\nu{}^P(r,n-1;s,n)]\}. \quad (13)$$

The approximation in Eq. (13) consists of having replaced factors $(1-f_s)$, giving the probability that a given state is unoccupied, by unity. The final state $k_r'$ can lie along all possible directions without violating either of the principles of conservation of momentum or energy, since for acoustical phonons of polarization $P$ we neglect the phonon energy in comparison to the hole energy whereas for optical phonons $\hbar\omega$ is constant and independent of $q$.

The specialization to specific vibrational modes may be deferred if $k_r'$ is expressed in terms of $\hbar\omega$, which at a later time can be set equal to zero for acoustical modes and $K\Theta$ for optical modes, where $\Theta$ is the temperature corresponding to the fundamental optical frequency. For the transitions from $\mathbf{k}_s$ to $\mathbf{k}_r'$ by phonon absorption and from $\mathbf{k}_r'$ to $\mathbf{k}_s$ by emission, we have, from conservation of energy, that

$$k_r'^2=(m_r/m_s)k_s^2(1+\hbar\omega/E_s). \quad (14)$$

For the transition from $\mathbf{k}_s$ to $\mathbf{k}_r'$ by phonon emission and $\mathbf{k}_r'$ to $\mathbf{k}_s$ by absorption, on the other hand,

$$k_r'^2=(m_r/m_s)k_s^2(1-\hbar\omega/E_s). \quad (15)$$

A given emission process, of course, can only take place if the energy of the hole in the initial state exceeds the phonon energy $\hbar\omega$.

Correspondingly, by use of Eq. (6), we may write (5) in the form

$$f_s(k_r')=e^{\pm(\hbar\omega/KT)}\{f^0(E_s)$$
$$+[df^0(E_s)/dE_s]a_s(E_s\mp\hbar\omega)\cos\theta_r\}, \quad (16)$$

where the upper and lower signs correspond to $k_r'$ as given by Eqs. (14) and (15), respectively.

In order to treat all phonon scattering terms at once, it is convenient to write the quantities $\mathcal{W}_\nu{}^P$ defined in Sec. 4 of the preceding paper in the form

$$\mathcal{W}_\nu{}^P(r,n';s,n)=(2\pi\hbar^3/Vm_rk_s)n'w_\nu{}^P(r,s)\mathcal{G}_\nu{}^P(r,s). \quad (17)$$

Comparison with Eqs. (4.18), (4.40), and (4.37) shows that

$$w_1{}^P(r,s)=C_1{}^2KTm_rk_s/4\pi u_P{}^2\rho\hbar^3n$$
$$\equiv(\hbar k_se\mathcal{E}/m_s)(m_s/m_1)(m_r/m_1)(u_L/u_P)^2(\beta_1/2n),$$
$$w_2{}^P(r,s)=C_4{}^2m_rk_s/\pi K\Theta\hbar\rho a_0{}^2$$
$$\equiv(\hbar k_se\mathcal{E}/m_s)(m_s/m_1)(m_r/m_1)\beta_2, \quad (18)$$
$$w_3{}^P(r,s)=C_3{}^2KTm_rk_s/4\pi\hbar^3\bar{u}^2\rho n$$
$$\equiv\tfrac{3}{2}(\hbar k_se\mathcal{E}/m_s)(m_s/m_1)(m_r/m_1)(T\Lambda/\Theta)(\beta_2/2n).$$

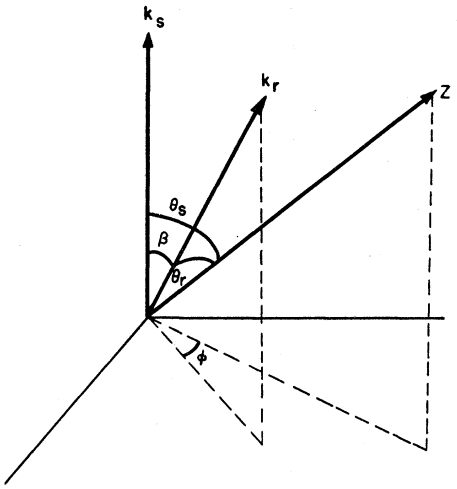


FIG. 1. Polar coordinate system used in transport calculations. The electric field is along the $z$ direction; $k_s$ and $k_r$ are wave numbers of holes in bands $s$ and $r$ before and after scattering.

In these definitions, we have used the fact that $n\approx n+1$ for acoustical modes. In addition, we have taken the opportunity to define the quantities $\beta_1$, $\beta_2$, and $\Lambda$ which will prove useful in the calculations to follow. The substitution of the preceding equations into (13) yields

$$(f_s)_{\nu,r}{}^P=(m_r/m_s)^{\frac{1}{2}}(w_\nu{}^P/2\pi)(df^0/dE_s)$$
$$\times\int_{-1}^{+1}dx\mathcal{G}_\nu{}^P(r,s)\Big\{n(1+\hbar\omega/E_s)^{\frac{1}{2}}\int_0^{2\pi}d\phi$$
$$\times[a_r(E_s+\hbar\omega)\cos\theta_r-a_s(E_s)\cos\theta_s]$$
$$+(n+1)(1-\hbar\omega/E_s)^{\frac{1}{2}}\int_0^{2\pi}d\phi$$
$$\times[a_r(E_s-\hbar\omega)\cos\theta_r-a_s(E_s)\cos\theta_s]\Big\}. \quad (19)$$

The integration over $\phi$ is readily performed with the help of Eq. (11). With the notation

$$R_\nu{}^P(s,r)=(m_r/m_s)^{\frac{1}{2}}\int_{-1}^{+1}x\mathcal{G}_\nu{}^P(r,s)dx,$$
$$S_\nu{}^P(s,r)=(m_r/m_s)^{\frac{1}{2}}\int_{-1}^{+1}\mathcal{G}_\nu{}^P(r,s)dx, \quad (20)$$

we obtain

$$(\dot{f}_s)_{\nu,r}{}^P=w_\nu{}^P(r,s)(df^0/dE_s)\cos\theta_s$$
$$\times\{n(1+\hbar\omega/E_s)^{\frac{1}{2}}[a_r(E_s+\hbar\omega)R_\nu{}^P(s,r)$$
$$-a_s(E_s)S_\nu{}^P(s,r)]+(n+1)(1-\hbar\omega/E_s)^{\frac{1}{2}}$$
$$\times[a_r(E_s-\hbar\omega)R_\nu{}^P(s,r)-a_s(E_s)S_\nu{}^P(s,r)]\}. \quad (21)$$

At this point, it becomes useful to distinguish between the rigid-ion (RI) and deformable-ion (DI) models for the terms $\nu=1$ and $P=L$ where the two models give different results in our treatment. In I, we introduced

TABLE I. Values of the integrals $R_\nu^P(s,r)$ and $S_\nu^P(s,r)$.

$R_1^L(1,1;1)=-44/225$
$R_1^L(2,2;1)=4/25$
$R_1^L(1,2;1)=(4/25)\alpha^{\frac{1}{2}}[(7/3-\alpha)A_1-\alpha A_2]$.
$R_1^L(1,1;0)=76/225$
$R_1^L(2,2;0)=-28/75$
$R_1^L(1,2;0)=(4/25)\alpha^{\frac{1}{2}}[(4\alpha-8/3)A_1-\alpha A_2]$.
$R_1^T(1,1)=R_1^T(2,2)=0$
$R_1^T(1,2)=(4/25)\alpha^{\frac{1}{2}}[-\frac{1}{2}(\alpha+1)A_1+\alpha A_2]$.
$R_\nu^P(s,r)=0$ for $\nu=2,3$; $r,s=1,2$; $P=L,T$.
$S_1^L(1,1;1)=164/225$
$S_1^L(2,2;1)=28/75$
$S_1^L(1,2;1)=(4/25)\alpha^{\frac{1}{2}}[7/3+(7/3-\alpha)B_1-\alpha B_2]$.
$S_1^L(1,1;0)=344/225$
$S_1^L(2,2;0)=56/25$
$S_1^L(1,2;0)=(4/25)\alpha^{\frac{1}{2}}[32/3+(4\alpha-8/3)B_1-\alpha B_2]$.
$S_1^T(1,1)=S_1^T(2,2)=4/75$
$S_1^T(1,2)=(4/25)\alpha^{\frac{1}{2}}[4/3-\frac{1}{2}(\alpha+1)B_1+\alpha B_2]$.
$S_2^L(1,1)=S_2^L(2,2)=\frac{1}{3}$
$S_2^L(1,2)=\frac{1}{3}\alpha^{\frac{1}{2}}$.
$S_2^T(s,r)=2S_2^L(s,r)$
$S_3^P(s,r)=\frac{2}{3}S_2^P(s,r)$.

a parameter $\eta$ having values in the range $0\leq\eta\leq1$ which distinguishes between the two models. In the limits $\eta=0$ and 1, the results correspond to the RI and DI models, respectively. The dependence on $\eta$ will be introduced explicitly by writing the quantities defined by Eq. (20) as $R_\nu^P(r,s;\eta)$ and $S_\nu^P(r,s;\eta)$. In considerations involving the RI model, we shall take $C_2$ to have the value given by Eq. (4.41) which is admittedly rough, but will serve to indicate the effects on the mobility.

The results of evaluating Eq. (20) are given in Table I. Some of these are most easily expressed in terms of the integrals:

$$A_1=\int_{-1}^{+1}(1-x^2)(x/\sigma)dx=(12\alpha^{\frac{3}{2}})^{-1}(3-2\alpha+3\alpha^2)+(8\alpha^2)^{-1}(1-\alpha)^2(1+\alpha)\log|(\alpha^{\frac{1}{2}}-1)/(\alpha^{\frac{1}{2}}+1)|,$$

$$A_2=\int_{-1}^{+1}(1-x^2)^2(x/\sigma^2)dx=(32\alpha^3)^{-1}\times[(1-\alpha)^2(5+6\alpha+5\alpha^2)\log|(\alpha^{\frac{1}{2}}-1)/(\alpha^{\frac{1}{2}}+1)|+\alpha^{\frac{1}{2}}(1+\alpha)(10-44\alpha/3+10\alpha^2)],\quad(22)$$

$$B_1=\int_{-1}^{+1}(1-x^2)\sigma^{-1}dx=(4\alpha^{\frac{3}{2}})^{-1}(1-\alpha)^2\times\log|(\alpha^{\frac{1}{2}}-1)/(\alpha^{\frac{1}{2}}+1)|+(1+\alpha)/2\alpha,$$

$$B_2=\int_{-1}^{+1}(1-x^2)^2\sigma^{-2}dx=2\alpha^{-\frac{1}{2}}A_1,$$

where $\sigma$ is defined by Eq. (4.25) of I. It is evident from Eq. (20) that

$$R_\nu^P(1,2)=\alpha R_\nu^P(2,1),$$
$$S_\nu^P(1,2)=\alpha S_\nu^P(2,1).$$

The explicit expressions of the $(\dot f_s)_{\nu,r}^P$ for the various $\nu$ can now be obtained from Eq. (15). For acoustical modes, corresponding to $\nu=1$ and 3, $\hbar\omega\approx0$ and $n\approx n+1$. Thus

$$(\dot f_s)_{1,r}^P=(\hbar k_s e\mathcal{E}/m_s)(m_r/m_1)(m_s/m_1)\times(u_L/u_P)^2\beta_1(df^0/dE_s)\cos\theta_s\times[a_r(E_s)R_1^P(s,r)-a_s(E_s)S_1^P(s,r)],\quad(23)$$

and

$$(\dot f_s)_{3,r}^P=(\tfrac{3}{2})(\hbar k_s e\mathcal{E}/m_s)(m_r/m_1)\times(m_s/m_1)(T/\Theta)\beta_2\Lambda(df^0/dE_s)\cos\theta_s\times a_s(E_s)S_3^P(s,r).\quad(24)$$

In the case of the optical modes ($\nu=2$),

$$(\dot f_s)_{2,r}^P=-(\hbar k_s e\mathcal{E}/m_s)(m_r/m_1)\times(m_s/m_1)\beta_2(df^0/dE_s)\cos\theta_s\phi(K\Theta/E_s)\times a_s(E_s)S_2^P(s,r),\quad(25)$$

where

$$\phi(x)=\begin{cases}n(1+x)^{\frac{1}{2}}+(n+1)(1-x)^{\frac{1}{2}} & \text{for } x<1\\ n(1+x)^{\frac{1}{2}} & \text{for } x>1.\end{cases}\quad(26)$$

It should be noted that the terms $R_\nu^P(s,r)(\nu=2,3)$ vanish and thus do not appear in Eqs. (24) and (25). This comes about because the angular distributions associated with the absolute squares of the matrix elements for scattering are symmetric about $\beta=90°$. This circumstance simplifies our problem greatly, since the terms $a_r(E_s\pm\hbar\omega)$, associated with optical modes, which would ordinarily appear in the Boltzmann equation are absent, and we avoid thereby having to solve a functional equation.

Finally, the field term $(\dot f_s)_F$ is

$$(\dot f_s)_F=-(e\mathcal{E}/\hbar)(\partial f/\partial k_z)=(\hbar k_s e\mathcal{E}/m_s)\cos\theta_s(df^0/dE_s).\quad(27)$$

It is to be emphasized that the dependence on the electric field $\mathcal{E}$ of Eqs. (23)–(25) is a result of the definition of $\beta_s$ and is purely fictitious. The reason for using this notation becomes apparent when these expressions, together with (27) are substituted into the Boltzmann equation and common nonzero terms are canceled. The results of this operation are most simply expressed in terms of the quantities

$$\gamma=u_L/u_T,\quad\vartheta=\Theta/T,\quad(28)$$

and

$$\mathcal{Q}_1(\eta)=-[R_1^L(1,1;\eta)-S_1^L(1,1;\eta)]-\gamma^2[R_1^T(1,1;\eta)-S_1^T(1,1;\eta)]+\alpha[S_1^L(1,2;\eta)+\gamma^2S_1^T(1,2;\eta)],$$
$$\mathcal{Q}_2(\eta)=-\alpha^2[R_1^L(2,2;\eta)-S_1^L(2,2;\eta)]-\alpha^2\gamma^2[R_1^T(2,2;\eta)-S_1^T(2,2;\eta)]+[S_1^L(1,2;\eta)+\gamma^2S_1^T(1,2;\eta)],\quad(29)$$
$$\mathcal{R}(\eta)=R_1^L(1,2;\eta)+\gamma^2R_1^T(1,2;\eta),$$
$$\mathcal{S}_1=[S_2^L(1,1)+S_2^T(1,1)]+\alpha[S_2^L(1,2)+S_2^T(1,2)],$$
$$\mathcal{S}_2=\alpha^2[S_2^L(2,2)+S_2^T(2,2)]+[S_2^L(1,2)+S_2^T(1,2)].$$

The Boltzmann equations (4) then become, upon writing $E_s=E$,

$$\begin{aligned}\{\beta_1\mathcal{Q}_1+\beta_2[\phi(K\Theta/E)+\Lambda/\vartheta]\mathcal{S}_1\}&\\ \times a_1(E)-\beta_1\alpha\mathcal{R}a_2(E)=1,&\\ \{\beta_1\mathcal{Q}_2+\beta_2[\phi(K\Theta/E)+\Lambda/\vartheta]\mathcal{S}_2\}&\\ \times a_2(E)-\beta_1\mathcal{R}a_1(E)=1.&\end{aligned}\tag{30}$$

These are coupled algebraic equations in $a_1(E)$ and $a_2(E)$. The fact that the coefficients $(df^0/dE_s)\cos\theta_s$ have canceled out demonstrates that as a result of our approximations involving the surfaces of constant energy and matrix elements for scattering, the postulated solution (5) is exact.

The special case in which $\beta_2=0$ will prove interesting. This means that we neglect optical modes as well as that portion of the acoustical modes arising from the vibrational phase difference between the two atoms of the unit cell. It is then seen from Eqs. (30) that

$$\begin{aligned}a_1(E)&=\beta_1^{-1}[\mathcal{Q}_2(\eta)+\alpha\mathcal{R}(\eta)]/\\ &\qquad[\mathcal{Q}_1(\eta)\mathcal{Q}_2(\eta)-\alpha\mathcal{R}^2(\eta)],\qquad(31)\\ a_2(E)&=\beta_1^{-1}[\mathcal{Q}_1(\eta)+\mathcal{R}(\eta)]/[(\mathcal{Q}_1(\eta)\mathcal{Q}_2(\eta)-\alpha\mathcal{R}^2(\eta)],\end{aligned}$$

which are independent of energy. Equation (10) then indicates that the relaxation time for each of the bands varies as $E^{-\frac{1}{2}}$. The current integral (9) can be given in closed form since the $a$'s are removed from the integral. Substitution of Eq. (31) into (9) and use of (3) gives

$$\mu=\mu_0(\mathcal{Q}_2+\alpha\mathcal{Q}_1+2\alpha\mathcal{R})/(\mathcal{Q}_1\mathcal{Q}_2-\alpha\mathcal{R}^2)\equiv\mu_0\Omega,\tag{32}$$

where

$$\mu_0=[4(2\pi)^{\frac{1}{2}}e\rho\hbar^4u_L^2]/[3m_1^{5/2}(KT)^{\frac{3}{2}}C_1^2(1+\alpha^{\frac{3}{2}})].\tag{33}$$

Equation (33), apart from a numerical constant involving the ratio of the effective masses $\alpha$, is the same expression as that obtained by Seitz and Bardeen and Shockley[2] for a single $s$-band. The mobility (32) thus exhibits the same $T^{-1.5}$ temperature dependence characteristic of the simpler theories. The factor multiplying $\mu_0$ in Eq. (32) will differ for the RI and DI models.

From the values of the constants to be evaluated in the next section, we shall see that the ratios $\alpha\mathcal{R}/\mathcal{Q}_1$, and $\mathcal{R}/\mathcal{Q}_2$ are both less than 0.1 for the DI and less than 0.03 for the RI model. Under these circumstances, the terms coupling Eqs. (30) can be neglected reasonably. With this approximation, we obtain the results

$$a_s(E)=\{\beta_1\mathcal{Q}_s+\beta_2[\phi(K\Theta/E)+\Lambda/\vartheta]\mathcal{S}_s\}^{-1}\quad s=1,2\tag{34}$$

when $\beta_2\neq0$. The neglect of the coupling terms greatly simplifies the last integration (9) and permits the formulation of approximate analytical techniques. In order to make absolutely sure of the resulting temperature dependence of the mobility we shall perform the integration numerically. We define

$$\begin{aligned}\rho_s&=\mathcal{Q}_s+(\beta_2/\beta_1)(\Lambda/\vartheta)\mathcal{S}_s,\\ \sigma_s&=(\beta_2/\beta_1)\mathcal{S}_s.\end{aligned}\tag{35}$$

The integral to be done may then be written

$$\begin{aligned}J_s=\int_0^1 dx[xe^{-\vartheta x}]/[\rho_s+n\sigma_s(1+x^{-1})^{\frac{1}{2}}]&\\ +\int_1^\infty dx[xe^{-\vartheta x}]/[\rho_s+n\sigma_s(1+x^{-1})^{\frac{1}{2}}&\\ +(n+1)\sigma_s(1-x^{-1})^{\frac{1}{2}}].&\end{aligned}\tag{36}$$

The resulting expression for the mobility is

$$\mu=\mu_0\vartheta^2(J_1+\alpha J_2),\tag{37}$$

and the ratio of currents carried by the two bands,

$$(j_1/j_2)=(J_1/\alpha J_2).\tag{38}$$

### 3. RESULTS AND DISCUSSION

To obtain the final numerical results, we shall now proceed to collect a set of values for the constants appearing in these calculations, some of which will reflect the approximations that have been made. For instance, we shall have to define appropriate sound velocities and elastic constants, in accordance with the assumption that the germanium lattice is a homogeneous, isotropic medium. This is done by considering the measured values of the longitudinal and transverse velocities in the [100], [110], and [111] directions and taking an average in which these directions are weighted in the ratios 3:6:4, respectively. The values $u_L=5.3\times10^5$ cm/sec and $u_T=3.3\times10^5$ cm/sec are thereby obtained. Using these values, we may determine a set of elastic constants that describe the hypothetical lattice under consideration. We obtain, with the density of germanium, $\rho=5.35$ g/cm$^3$,

$$\begin{aligned}c_{11}&=\rho u_L^2=1.5\times10^{12}\text{ dynes/cm}^2,\\ c_{44}&=\rho u_T^2=0.58\times10^{12}\text{ dynes/cm}^2.\end{aligned}$$

The third elastic constant, $c_{12}$, is gotten from the relationship $c_{12}=c_{11}-2c_{44}$, which describes an elastically isotropic medium. We find

$$c_{12}=0.34\times10^{12}\text{ dynes/cm}^2.$$

Substitution of these values into the expression for $\delta$ defined by Eq. (4.5) of I yields $\delta=0.7$. It will be recalled that the assumption of interaction with nearest and next-nearest neighbors was used in calculating $\delta$. In this connection, it should be noted that the use of only nearest neighbors produces results that are fundamentally incompatible with the assumption of an elastically isotropic medium, since in that case the elastic constants satisfy the additional constraint

[2] F. Seitz, Phys. Rev. **73**, 549 (1948); J. Bardeen and W. Shockley, Phys. Rev. **80**, 72 (1950).

$4c_{11}(c_{11}-c_{44})=(c_{11}+c_{12})^2$. Combination of the two conditions yields the following two rather absurd sets of relationships between the elastic constants: $c_{44}=0$, $c_{12}=c_{11}$, and $2c_{11}=c_{44}$, $c_{12}=-3c_{11}$. The question, however, remains as to whether the value of $\delta$ obtained by the inclusion of next nearest neighbors is reliable, since no calculations of measurable quantities like the specific heat have yet been done for germanium using this approximation. The calculations of Hsieh[3] have considered only nearest neighbor interactions, but have obtained agreement with the experimental specific heat within about 10%,

The same sort of difficulty arises in the determination of the fundamental optical frequency $\omega=K\Theta/\hbar$. This quantity is directly measurable as the fundamental Raman frequency. The value 1332 $cm^{-1}$ has been obtained in diamond. On the other hand, the infrared lattice absorption spectrum occurs in the range 2892 to 3612 $cm^{-1}$ which is roughly twice the optical frequency. According to Lax and Burstein,[4] this spectrum may be associated with two-phonon processes which produce second-order electric moments. Turning now to germanium, we find the Raman frequency as yet undetermined experimentally. The calculations of Smith[5] as applied to germanium, however, yield the value $\omega=390$ $cm^{-1}$ ($\Theta=560°K$). This value falls into the spectral range associated with the infrared lattice absorption, extending between 345 and 640 $cm^{-1}$. This spectrum contains an apparently impurity-insensitive peak at 345 $cm^{-1}$ whose intensity is much greater than the remaining structure and which is without analog in the diamond spectrum. The temptation is therefore strong to interpret this as the fundamental optical frequency. If we argue, however, that the gross features of the spectra should be alike for diamond and germanium because of their similar atomic structure, then we are led to the conclusion that the fundamental optical frequency should occur somewhere around $\Theta=300°K$ and that Smith's calculations do not give accurate results when applied to the optical modes of germanium. Since we are unable to resolve this dilemma, we shall present results for two optical mode temperatures, $\Theta=300$ and 500°K and contrast the behavior of the mobility so obtained with temperature.

Only two further numerical constants are required. These are the edge-length of the fundamental face-centered cube, $2a_0=5.62\times10^{-8}$ cm, and the value of $\bar{u}$, defined by Eq. (4.27) of I, which is $4.1\times10^5$ cm/sec.

We shall first discuss the results for the mobility and current density in the case when $C_3=C_4=0$. This case is of interest since it does not involve optical modes, nor the acoustical term representing phase differences between the two atoms in a unit cell. It has been thought unlikely that the introduction of optical modes could explain the behavior of the mobility because the strong temperature dependence associated with the component terms (3.2) of I would not give a straight line on a plot of $\log\mu$ *vs* $\log T$. This argument is refuted by the present calculations. Furthermore, as pointed out by Brooks,[6] it is hard to reconcile the galvanomagnetic effects with a relaxation time having an energy dependence that is very different from $E^{-\frac{1}{2}}$. This means that $a_s(E)$ should be nearly independent of energy. The relaxation time obtained here depends on energy in a rather more complicated way. The question as to whether this variation is too rapid to explain the magnetoresistance requires detailed treatment and will not be considered in this paper.

In discussing these results, it will also be of interest to compare the values obtained on the basis of the RI and DI models. We can already see from Eq. (32) that both models must give a mobility having a $T^{-1.5}$ dependence. To obtain values for $\Omega$ defined by that equation for the two models, we use the numbers giving $\mathcal{Q}_1$, $\mathcal{Q}_2$, and $\mathcal{R}$ in the two cases, as obtained from Eq. (29). These are 62.1, 178, 0.200, respectively for the RI model and 11.9, 22.9, −0.184 for the DI model. It is now seen that the ratios $\alpha\mathcal{R}/\mathcal{Q}_1$ and $\mathcal{R}/\mathcal{Q}_2$ are small, as maintained in the preceding section. Substituting the values of $\mathcal{Q}_1$, $\mathcal{Q}_2$, and $\mathcal{R}$ into Eq. (32) gives

$$\begin{aligned}\mu(\text{cm}^2/\text{volt-sec})&=4.6\times10^9/T^{1.5}C_1^2(\text{ev}) \quad \text{DI}\\ &=7.0\times10^8/T^{1.5}C_1^2(\text{ev}) \quad \text{RI}\end{aligned} \tag{39}$$

for the two models. The kinetic energy $C_1$ is to be expressed in electron volts and the mobility in the conventional units of $cm^2$/volt-sec. For the same $C_1$ and $T$, the mobility obtained from the DI model is always greater than that obtained from the RI model, as is to be expected from the larger amount of scattering associated with the RI model shown in Fig. 2 of I. It is interesting that for roughly the same value of $C_1$, the DI and RI models represent upper and lower bounds respectively for the mobility in the lattice-scattering range. One finds that $C_1=10.6$ ev matches the theoretical and experimental mobilities at 50°K for the DI model, and 8.7 ev matches the mobilities at 300°K for the RI model. The magnitude $C_1\approx10$ ev is reasonable, for the first ionization potential of atomic germanium is about 8 ev and from the virial theorem for a Coulomb potential, it follows that the corresponding kinetic energy is about 8 ev. It is thus possible to obtain the correct value of the mobility at any temperature in the lattice-scattering range for a reasonable $C_1$, provided we pick an appropriate value of $\eta$. The *magnitude* of the mobility at any temperature in the lattice-scattering range therefore can be understood. The

[3] Y. C. Hsieh, Phys. Rev. **85**, 730 (1952).
[4] M. Lax and E. Burstein, Phys. Rev. **97**, 39 (1955).
[5] Helen M. J. Smith, Trans. Roy. Soc. (London) **A241**, 105 (1948).
[6] H. Brooks, in *Advances in Electronics* (Academic Press, Inc., New York, 1956), Vol. 7.

problem is to explain the observed temperature dependence, since $\eta$ cannot vary with temperature.

The mobilities obtained from the two models using the values of $C_1$ given above are plotted in Fig. 2. The experimental mobility is shown for comparison. In addition, we have plotted the mobilities resulting from both models when either longitudinal or transverse phonons alone contribute to the scattering. It is seen that transverse phonons influence the mobility only slightly in the case of the RI model, whereas both types of phonons are roughly equally effective in the case of the DI model, with the longitudinal phonons dominating somewhat.

The mobility ratios for the two bands are given by

$$\mu_1/\mu_2=\alpha^{\frac{1}{2}}a_1/a_2. \tag{40}$$

We find the values $\mu_1/\mu_2=8.1$ for the RI model and 5.2 for the DI model. In the simple situation where the wave functions of both bands have $s$-symmetry and the only scattering mechanisms are intraband scattering for carriers in the heavy-mass band and interband scattering for carriers initially in the light-mass band, the mobility ratio should equal the inverse ratio of the effective masses, that is, $\mu_1/\mu_2=\alpha$. This result follows from the fact that the relaxation times for carriers of both bands are the same in this case. It is seen that the RI result agrees closely with the preceding mobility ratio, whereas the DI result is rather different. The conclusions obtained from the RI model concerning the importance of transverse modes and the ratio $\mu_1/\mu_2$ agree rather well with those of Brooks[6] whose treatment is based on the deformation potential theory without including optical modes.

Let us next consider the relative importance of the two bands in the conduction process by computing the current ratio $j_1/j_2$. This quantity is given by

$$j_1/j_2=a_1/\alpha a_2. \tag{41}$$

One might expect the lighter holes to be more effective current carriers than the heavier holes, since, if the bands were independent, and the matrix elements for scattering in each band the same, one would have $j_1/j_2=(n_1/n_2)(\mu_1/\mu_2)=\alpha\approx 8$. In fact, however, the matrix elements for the different scattering mechanisms are considerably different, as has already been seen from Figs. 1 and 2 of I. One notes in particular that for intraband scattering in the DI model the light holes are predominantly scattered backwards, whereas the heavy holes are scattered forward. The opposite is true of the RI model. If interband scattering is turned off by setting $\mathfrak{R}=S_1{}^P(r,s)=0$, we find the current ratio to be $j_1/j_2=2.6$ for the DI model and 16 for the RI model. These values reflect the fact that in the first case the importance of the light holes is diminished and in the second case it is enhanced. The presence of interband scattering will affect chiefly the holes of light mass by tending to scatter them into the other band with its associated large density of states. For interband scattering alone, we find $j_1/j_2\sim 0.001$ and 0.02 for the DI and RI models, respectively. The total current ratios are 0.23 and 0.37, the larger value pertaining to the RI model.

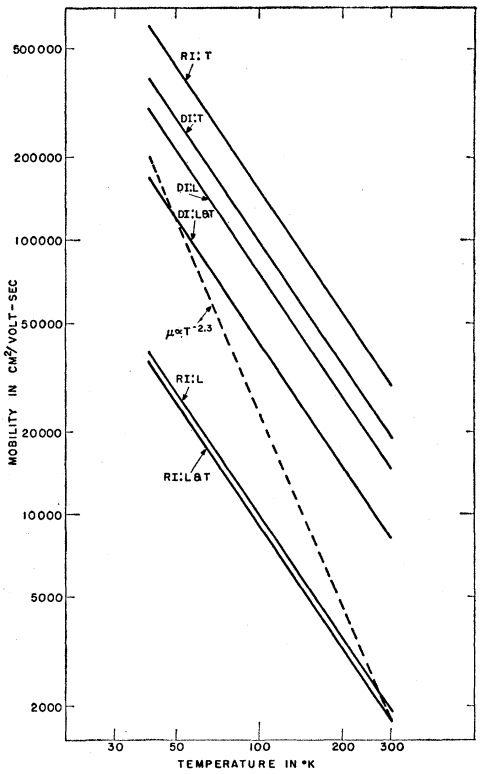


FIG. 2. The hole mobility *versus* temperature obtained from the DI and RI models for $C_4=0$. The dashed curve represents the experimental mobility. The curves labeled DI:L and T and RI:L and T represent the calculated mobility, resulting from scattering by longitudinal (L) and transverse (T) phonons, matched at 50°K for the DI model and at 300°K for the RI model. The values of $C_1$ used are 10.6 ev for the DI and 8.7 ev for the RI model. The remaining curves show the mobilities, using these values of $C_1$, when either longitudinal or transverse phonons alone produce the scattering.

We shall now give the final results for the mobility and current ratios when the terms involving $C_3$ and $C_4$ are included. These results were calculated numerically from Eqs. (37) and (38). The theory contains two constants, $C_1$ and $C_4$, which are not related to each other in any simple way. Both depend on the germanium wave functions and potential and must be computed directly from these quantities. Since this has not been done, we shall give the results for various values of the ratio $C_4/C_1$. For purposes of comparison, the computed values of the mobility were matched with the experimental value[7] at 50°K. For a given ratio $C_4/C_1$, the matching thus determines both constants. The results are shown in Figs. 4–7 for the RI and DI models, assuming that

[7] F. J. Morin, Phys. Rev. **93**, 62 (1953); M. B. Prince, Phys. Rev. **92**, 681 (1953). F. J. Morin and J. P. Maita, Phys. Rev. **94**, 1525 (1954).

$\Theta=300°K$ or $500°K$ in each case. The values of $C_1$ corresponding to the various ratios $C_4/C_1$ are given in the figure captions. We have chosen the ratios $C_4/C_1=0$, 1, 2, 5, and $\infty$ as representive of the effect produced by varying the magnitude of optical modes. The value $C_4/C_1=0$ corresponds to the curve having the $T^{-1.5}$ dependence; the value $\infty$ corresponds to having set $C_1=0$. We have represented the experimental mobility and the curve obeying a $T^{-1.5}$ dependence by dashed lines.

One observes that the ratio $C_4/C_1=\infty$ will correspond to the most rapid possible temperature dependence provided that the neglected interference terms in $C_1C_3$ and $C_1C_2$ of I, Eq. (4.17), are small. We have estimated the importance of these terms by calculating the matrix elements for scattering from a [100] direction to a final state in a plane containing all three principal directions for which $k_x'=k_y'$. These results depend only on the angle of scattering $\beta$. If we regard these scattering cross sections as typical of the scattering into any other direction, we may then compute the mobility. It should be remembered, however, that these interference terms may be either positive or negative since the relative signs of $C_1$ and $C_3$ are unknown. Figure 3 shows the corrections involved for interference terms of either sign in the case of both DI and RI models when $C_4/C_1=2$ and $\Theta=500°K$. As before, the experimental and calculated mobilities have been matched at 50°K. The effect of the interference terms is seen to be fairly small for the DI model and negligible for the RI model. The following conclusions thus are unaffected in any essential way by the neglect of the interference terms.

The most striking feature of Figs. 4–7 is that even if $C_4\gg C_1$, the observed mobility cannot be explained for $\Theta=500°K$. This is due to the fact that the terms involving $C_4$ alone include an acoustical term whose magnitude is proportional to $\delta^2$, so that optical modes are always accompanied by a term having a $T^{-1.5}$ dependence. Optical modes, acting alone, give rise to a more rapidly varying temperature dependence as we shall see later. It should be noted that in our treatment there is no difference between the curves labeled $C_4/C_1=\infty$ pertaining to the RI and DI models since we have treated the terms in the electron-phonon interaction involving $C_3$ and $C_4$ only in the RI approximation. There is a difference, however, for $C_4/C_1=1$, 2, 5. For any given ratio the DI model always produces the more rapid temperature variation. This can be understood if one remembers that the matrix elements involving $C_1$ were larger for the RI model. For $\Theta=300°K$ there are values

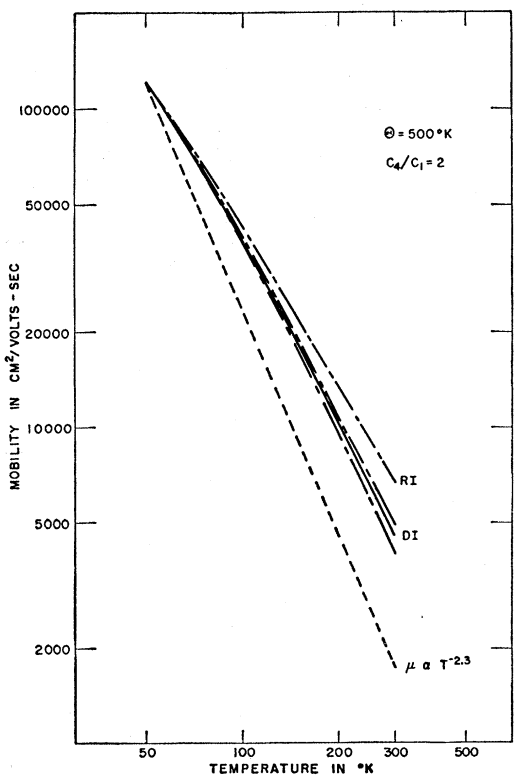


FIG. 3. Modification of the mobility as a function of temperature produced by the interference terms. The dot-dashed curves represent upper and lower bounds when the interference terms are included. The solid line represents the mobility when the interference terms are neglected. All three curves coincide on the scale of this graph for the RI model.

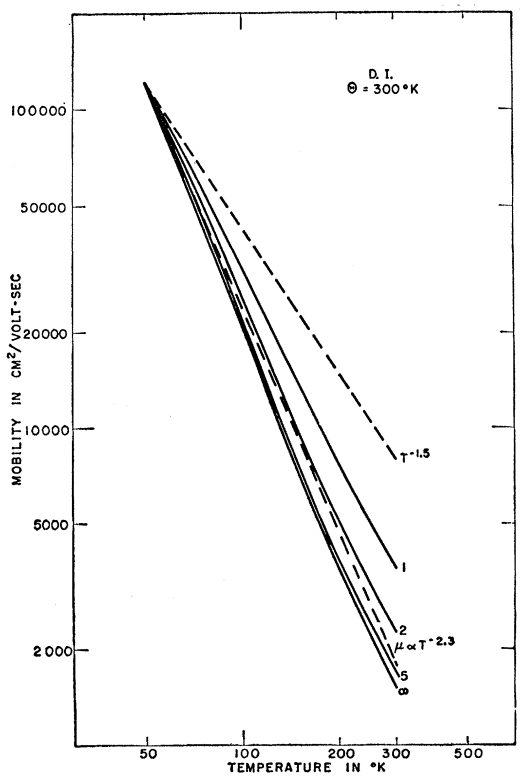


FIG. 4. The hole mobility *versus* temperature for the DI model, $\Theta=300°K$, matched with the experimental curve, labeled $\mu$, at 50°K, for $C_4/C_1=1,2,5\infty$. The values of $C_1$ in ev corresponding to these ratios are 9.1, 6.6, 3.2, 0.

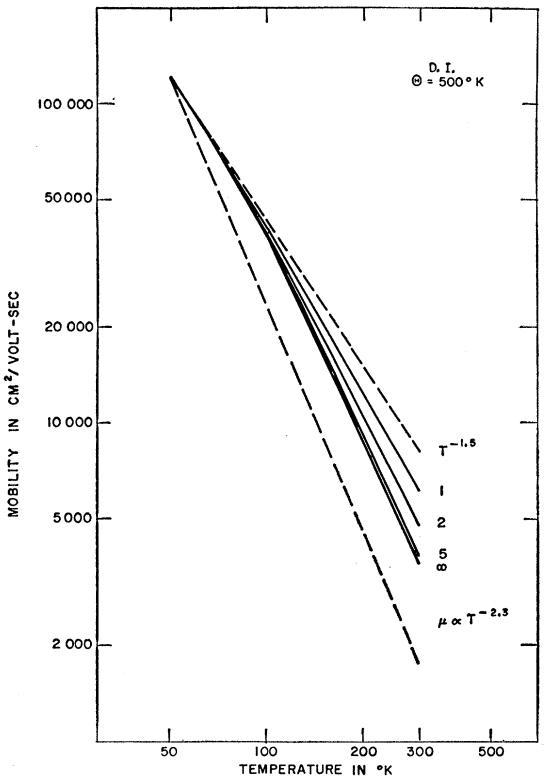


FIG. 5. The hole mobility *versus* temperature for the DI model, $\Theta=500°K$, matched with the experimental curve, labeled $\mu$, at 50°K, for $C_4/C_1=1,2,5,\infty$. The values of $C_1$ in ev corresponding to these ratios are 9.2, 6.9, 3.4, 0.

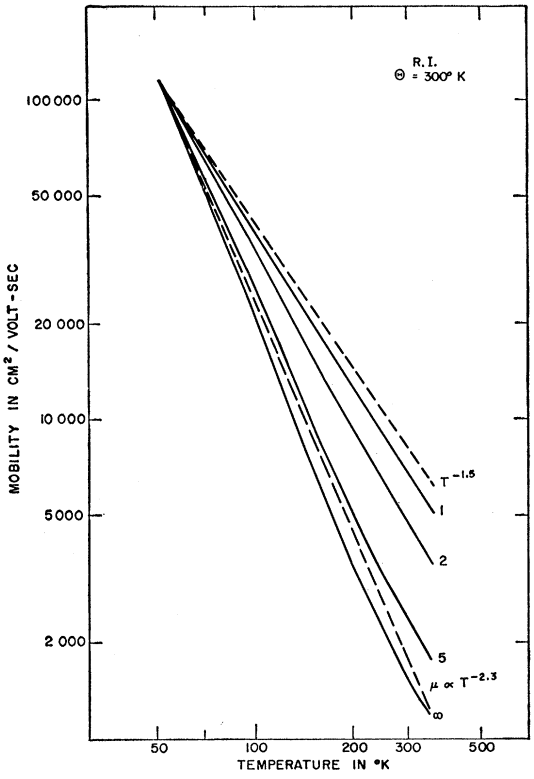


FIG. 6. The hole mobility *versus* temperature for the RI model, $\Theta=300°K$, matched with the experimental curve, labeled $\mu$, for $C_4/C_1=1,2,5\infty$. The values of $C_1$ in ev corresponding to these ratios are 3.9, 3.6, 2.6, 0.

$C_4/C_1$ for both models which will fit the experimental mobility quite satisfactorily. The best fit, however, requires a smaller value of the ratio $C_4/C_1$ if the DI model has been used. $C_4/C_1$ is then between 2 and 5, whereas the ratio is greater than 5 in the other case.

We note that the curvature of the lines drawn through the computed points in Figs. 4–7 is rather small. This fact is illustrated somewhat more dramatically in Fig. 8, where the results for the DI model with $C_4/C_1=2$ ($C_1=6.6$ ev, $C_4=13.3$ ev) and $\Theta=300°K$ are analyzed in some detail. We have taken the computed points and passed the best straight line, having slope $-2.25$, through them. The points are seen to fit a straight line quite well.* To show the relative importance of the terms involving $C_4$ and $C_1$, curves have been drawn for $C_1=0$, $C_4=13.3$ ev, and $C_1=6.6$ ev, and $C_4=0$. The curve having $C_1=0$ and $\delta=0.7$ provides a reasonable approximation to the resultant curve between 100°K and 300°K, thus showing that the term involving $C_4$ in the mobility is rather more important than that in $C_1$ for these particular values of the constants. The influence of the optical modes in the $C_4$ term is illustrated by a further curve for which $C_1=0$, $C_4=13.3$ ev, and $\delta=0$, representing the contribution of optical modes alone. The curvature is rather large, but is seen to be reduced considerably when $C_1$ and $C_4$ are as before and $\delta=0.7$.

Since the calculated mobility for the ratio $C_4/C_1=2$ agrees rather well with the observed mobility, the question arises whether the magnitude of $C_4/C_1$ is reasonable. This question can be answered unambiguously only by a detailed calculation of these constants. Qualitatively speaking, however, one might think on the one hand that $C_4$ should be smaller than $C_1$ since for a spherical atomic cell and a potential having spherical symmetry, $C_4$ vanishes whereas $C_1$ does not. On the other hand, the integration of functions over a tetrahedral cell that, losely speaking, might be considered prototypes for the germanium wave functions and potential suggest that ratios $C_4/C_1$ having the magnitude required to explain the mobility temperature dependence can be obtained.[8] The values of $C_1$ that arise in Figs. 4–7 appear reasonable.

* Qualitatively similar conclusions concerning the combination of acoustical and optical mode scattering have been obtained by W. A. Harrison [Phys. Rev. (to be published)].

[8] We have calculated $C_2$ and $C_4$, defined respectively by Eqs. (4.10) and (4.11) of I, putting $|\epsilon_i\rangle=x$, $y$, $z$ for $i=1$, 2, 3, $V=-\sin^2(\pi x/2)\sin^2(\pi y/2)\sin^2(\pi z/2)$, and $a_0=2$. The coordinate axes coincide with the cubic axes of the crystal, and the origin coincides with the atom at the center of the atomic cell forming the region of integration which was chosen to be tetrahedral. Assuming that $C_2=-2C_1$, we found that $C_4/C_1=+3.5$.

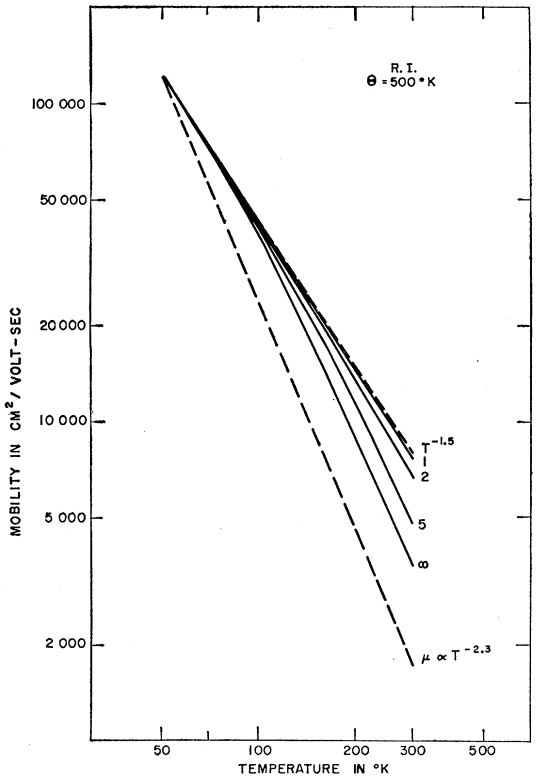


FIG. 7. The hole mobility *versus* temperature for the RI model, $\Theta=500°K$, matched with the experimental curve, labeled $\mu$, for $C_4/C_1=1,2,5,\infty$. The values of $C_1$ in ev corresponding to those ratios are 4.0, 3.7, 2.7, 0.

The numerical integrations that were necessary to calculate the mobility, also permit the determination of the current ratios $j_1/j_2$. Since $a_1$ and $a_2$ are functions of energy, the current ratio will depend on temperature. The variation with temperature of $j_1/j_2$, however, is small. Asymptotically the high- and low-temperature current ratios are given by Eq. (41) with

$$a_s(E)=[\beta_1 \mathcal{Q}_s+\beta_2 F(\vartheta) S_s/\vartheta]^{-1}, \tag{42}$$

where

$$F(\vartheta)=\Lambda \quad \text{for } \vartheta\gg 1,$$
$$=2+\Lambda \quad \text{for } \vartheta\ll 1.$$

For the DI model, the ratio $j_1/j_2$ increases by less than 15% over the entire range of temperatures, whereas for the RI model it decreases by less than 3%. The contrasting behavior with temperature of the two models may not be significant since the difference between the high- and low-temperature limits of $j_1/j_2$ is caused entirely by optical modes which have been treated in the RI approximation only. The results concerning the current ratios may be summarized with the observation that the values of $j_1/j_2=0.37$ and 0.23 obtained on the basis of the RI and DI models when $C_4=0$, respectively, represent the maximum and minimum possible values.

If one believes that the contribution of optical modes required to produce agreement between the theoretical and experimentally observed hole mobility is unreasonably large, then one must ask what other processes, not treated in these calculations, could account for the temperature dependence. It has already been pointed out that $k^4$ terms in the energy are too small to affect the mobility appreciably. We shall consider briefly some further possibilities.

The first possibility is an explicit variation of the effective mass with temperature. This can occur by means of the interaction with the phonon field: a hole emits and reabsorbs the same phonon. Physically, this implies that the motion of the hole through the crystal is retarded by a cloud of virtual phonons surrounding it. The effective mass is thereby increased from a value $m_s$ to $m_s^*$. It is this renormalized effective mass $m_s^*$ which should appear in the calculated expression for the mobility in place of $m_s$. The mass $m_s^*$ will increase with temperature, since the probability of emitting and reabsorbing a phonon is proportional to the number of phonons in the field. The mobility thus decreases more rapidly with increasing temperature. However, calculations using second-order perturbation theory[9] show that the change of effective mass is insignificantly small. The fractional change of mass is of order $10^{-5}$ between 0°K and room temperature. The possibility that higher order terms may be important in the perturbation series has been examined by Fulton,[10] who finds them negligible. He has shown that the coupling constant characterizing the electron-phonon interaction in semiconductors is $10^{-5}$, thus demonstrating the validity of perturbation theory in treating this interaction.

Another effect producing a variation of the effective mass is the change of band gap with temperature. The effective mass is theoretically determined from the quantities $L$, $M$, and $N$ defined by Eq. (2.4) of I, and the temperature dependence arises from variation of the energy denominators $(E_0-E_{\lambda\alpha})$. It might be pointed out that, in addition, the shift of the band edges with temperature should cause the coupling constants $C_1,\cdots,C_4$ to change. A rough estimate shows that these two effects are small and seem to change the temperature dependence of the mobility in a direction which would worsen the agreement between theory and experiment.

A still further possibility that has been considered is the change in the temperature dependence of the mobility produced by nonlinear vibrations of the lattice. In this case, the electron-phonon interaction Hamiltonian contains terms proportional to the square and higher powers of the displacement whose effect would be to create or annihilate two or more phonons

[9] H. Ehrenreich, Ph.D. thesis, Cornell University, 1955 (unpublished).
[10] T. Fulton (private communication).

at a time. This problem has been considered by Enz[11] who finds that the exponent of the temperature dependence is shifted in the right direction if these terms are important.

In this connection, it should be noted that the interaction Hamiltonian (3.4) which is linear in the atomic displacements, can also give rise to higher order terms in the electron-phonon interaction. The operator $H^I$ may act several times leading to the simultaneous creation or annihilation of more than one phonon. These higher order terms must not be considered since the recoil of a hole during a given scattering mechanism can be neglected. It has been shown[9] that in this case first-order perturbation theory gives the probability that *at least* one phonon is emitted or absorbed during a scattering process, and not exactly one, as is generally supposed. A first-order perturbation calculation thus includes automatically the effects of such processes on transport theory.

In conclusion, we shall comment briefly on the careful, but unsuccessful efforts[12] to observe light holes independently of the heavy holes by means of the drift technique.[13] It would be possible to effect a spatial or time separation between the two pulses in a drift experiment if the relaxation time due to all interband processes were less than the drift time, which was $5\times10^{-5}$ sec in Harrick's experiment. However, since for the light holes the interband scattering is dominant, a relaxation time of the order of $10^{-12}$ sec is to be associated with this process for the light holes, thus demonstrating the impossibility of observing them experimentally by this technique. One should not be misled by the fact that it was possible to neglect the terms in Eq. (30) which couple the two bands mathematically, to the conclusion that the carriers remain in one band. The quantities $\mathcal{Q}_s$ defined in Eq. (38) contain very important contributions from interband scattering. These terms in $\mathcal{Q}_s$ can be interpreted in the steady state as representing scattering within band $s$ in the sense that a carrier scattered into the other band is immediately replaced by a carrier resulting from an inverse interband transition. If now the two pulses were spatially separated, then the pulse corresponding to carriers in band $s$ could not be so replenished. Therefore, both the interband terms in $\mathcal{Q}_s$ as well as the coupling term $\mathcal{R}$ must be negligible if the two kinds of holes are to be observed independently in a drift experiment.[14]

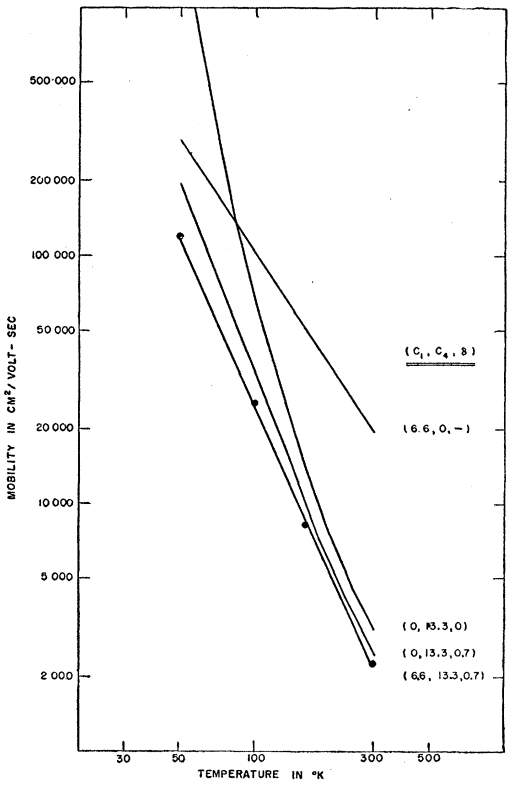


FIG. 8. Analysis of the curve, appearing in Fig. 4, for $C_4/C_1=2$ ($C_1=6.6$, $C_4=13.3$, $\delta=0.7$). A straight line has been passed through the computed points shown in the figure. The remaining curves show the effects of setting one or more of the quantities $C_1$, $C_4$, and $\delta$ equal to zero.

## 4. ACKNOWLEDGMENTS

We have benefited from conversations with H. Brooks, E. O. Kane, and F. S. Ham. We are indebted to H. Brooks for a copy of his manuscript in advance of publication, to P. V. Gray for his indispensable help with the numerical calculations, and to W. W. Piper and Elise Kreiger for programing the numerical integrations.

[11] Ch. Enz, Physica **20**, 983 (1954); Helv. Phys. Acta **27**, 199 (1954).

[12] N. J. Harrick, Phys. Rev. **98**, 1131 (1955).

[13] See also E. S. Rittner, Phys. Rev. **101**, 1291 (1956).

[14] The approximation corresponding to uncoupled bands has been used by Willardson, Harman, and Beer [Phys. Rev. **96**, 1512 (1954)] to analyze data of the transverse Hall and magnetoresistance effects in $p$-type germanium. It should be noted that their treatment has only assumed the two bands to be uncoupled mathematically. The present calculations show that their approximation does not imply that interband scattering has been completely or even appreciably neglected.